

Analyses of elastic waves in Aluminum/Barium sodium niobate and Quartz/Epoxy phononic structures

Zi-Gui Huang, Tsung-Tsong Wu¹ and S. Lin

Institute of Applied Mechanics, National Taiwan University,
Taipei 106, Taiwan

Keywords: Surface wave, Bulk wave, Periodic structures, Phononic crystal, Band gap

Abstract. This study was aimed at using the theory for two-dimensional phononic crystal consisting of materials with general anisotropy to calculate the band gaps phenomena in Aluminum/Barium sodium niobate (Y-cut) with hexagonal lattice and Quartz/Epoxy with square lattice phononic structures. Wave propagation properties of solids in which the periodic modulation occurs along the bounding surface has been discussed in this paper. Especially surface and bulk acoustic wave properties of solids were studied in both square and hexagonal lattices consisting of isotropic, trigonal, and orthorhombic symmetry materials. From the previous laboratory study, we confirmed that the widths of the frequency band gap were strongly affected by the filling ratio, density, and elastic constants matching ratios. In this study, the results have shown that surface wave band gaps could be found along a specific direction. In the materials we investigated in this paper, we found that there is no full band gap for surface waves. Instead, full band gap for bulk acoustic wave can be obtained for transverse polarization mode. Results of this paper can serve as a basis for both numerical and experimental investigations of phononic crystal related structures.

Introduction

The existence of complete band gaps of electromagnetic waves in photonic structures extending throughout the Brillouin zone has demonstrated a variety of fundamental and practical interests.[1,2] This has led to a rapid growing interests in the analogous acoustic effects in periodic elastic structures called the phononic crystals. Surface wave propagation on layered superlattices with traction free surface parallel to the layers has been explored extensively in the past.[3] However, investigations on surface wave properties of solids in which the periodic modulation occurs on the traction free surface has not started until recently.[4-8] Vignes *et al.*[4,5] studied experimentally the surface waves generated by a line-focus acoustic lens at the water-loaded surfaces of a number of two-dimensional superlattices that intersect the surface normally. Propagation of Scholte-like acoustic waves at the liquid-loaded surfaces of period structures has also been studied.[6]

The superlattices considered in Refs.[4-6,8] are of isotropic materials. As for superlattices consist of anisotropic materials, Tanaka and Tamura [7] reported detail calculations for surface waves on a square superlattice consisting of cubic materials (AlAs/GaAs) and many salient features of surface waves in two-dimensional superlattices have been described. In addition, Tanaka and Tamura[8] also reported detail calculations for surface waves on a hexagonal superlattice consisting of isotropic materials (Al/polymer).

For the analysis of bulk acoustic waves [9-15], Kushwaha *et al.*[9] reported the first full band-structure calculations of the transverse polarization mode for periodic, elastic composite. In the Ref.[10], Kushwaha *et al.* calculated the band structures for the transverse polarization modes of nickel alloy cylinders in aluminum alloy host, and vice versa. They also investigate the dependence of spectral gap on the filling fraction and on the material parameters. Kafesaki *et al.*[11] reported the multiple-scattering theory (MST method) for three-dimensional periodic acoustic composites.

¹ Corresponding author: wutt@spring.iam.ntu.edu.tw

Garcia-Pablos *et al.*[12] used the FDTD method to interpret experimental data for two-dimensional systems consisting of cylinders of fluids (Hg, air, and oil) inserted periodically in a finite slab of Al host. Psarobas and Stefanou[13] calculated the band structure of a phononic crystal consisting of complex and frequency dependent Lamé' coefficients. Zhengyou Liu *et al.*[14] extended the multiple-scattering theory for elastic waves by taking into account the full vector character, and presented a comparison between theory and ultrasound experiment for a hexagonal-close-packed array of steel balls immersed in water. Jun Mei *et al.*[15] reported the same method in Ref.[16] to extend the method in the case of cylinders. However, the bulk waves analysis in phononic structures among the Refs.[9-15] are of isotropic materials only.

In this paper, we extended Ref.[7] to study phononic band gaps of elastic/acoustic waves in two-dimensional Aluminum/Barium sodium niobate (Y-cut) ($\text{Ba}_2\text{NaNb}_5\text{O}_{15}$) with hexagonal lattice and Quartz/Epoxy with square lattice phononic structures. The explicit formulations of the plane harmonic bulk wave and the surface wave dispersion relations in such a general phononic structure are discussed based on the plane wave expansion method.

Equations of Motion of 2-D Phononic Crystals

In an inhomogeneous linear elastic anisotropic medium with no body force, the equation of motion for the displacement vector $\mathbf{u}(\mathbf{r}, t)$ can be written as

$$\rho(\mathbf{r})\ddot{u}_i(\mathbf{r}, t) = \partial_j [C_{ijmn}(\mathbf{r})\partial_n u_m(\mathbf{r}, t)] \quad (1)$$

where $\mathbf{r} = (\mathbf{x}, z) = (x, y, z)$ is the position vector, $\rho(\mathbf{r})$, $C_{ijmn}(\mathbf{r})$ are the position-dependent mass density and elastic stiffness tensor, respectively. In the following, we consider a phononic crystal composed of a two dimensional periodic array (x - y plane) of material A embedded in a background material B . Due to the spatial periodicity, the material constants, $\rho(\mathbf{x})$, $C_{ijmn}(\mathbf{x})$ can be expanded in the Fourier series with respect to the two-dimensional reciprocal lattice vectors (RLV), $\mathbf{G} = (G_1, G_2)$, as

$$\rho(\mathbf{x}) = \sum_{\mathbf{G}} e^{i\mathbf{G}\cdot\mathbf{x}} \rho_{\mathbf{G}} \quad (2)$$

$$C_{ijmn}(\mathbf{x}) = \sum_{\mathbf{G}} e^{i\mathbf{G}\cdot\mathbf{x}} C_{\mathbf{G}}^{ijmn} \quad (3)$$

where $\rho_{\mathbf{G}}$ and $C_{\mathbf{G}}^{ijmn}$ are the corresponding Fourier coefficients.

On utilizing the Bloch theorem and expanding the displacement vector $\mathbf{u}(\mathbf{r}, t)$ in Fourier series for bulk wave analysis, we have

$$\mathbf{u}(\mathbf{r}, t) = \sum_{\mathbf{G}} e^{i\mathbf{k}\cdot\mathbf{x} - i\omega t} (e^{i\mathbf{G}\cdot\mathbf{x}} \mathbf{A}_{\mathbf{G}} e^{ik_z z}) \quad (4)$$

where $\mathbf{k} = (k_1, k_2)$ is the Bloch wave vector, ω is the circular frequency and k_z is the wave number along the z -direction, $\mathbf{A}_{\mathbf{G}}$ is the amplitude of the displacement vector. We note that as the component of the wave vector k_z equals to zero, Eq. (6) degenerates into the displacement vector of a bulk acoustic wave.

Substituting Eqs. (2), (3) and (4) into Eq. (1), and after collecting terms systematically, we obtain the generalized eigenvalue problem

$$(\mathbf{A}k_z^2 + \mathbf{B}k_z + \mathbf{C})\mathbf{U} = 0 \quad (5)$$

where \mathbf{A} , \mathbf{B} and \mathbf{C} are $3n \times 3n$ matrices and are functions of the Bloch wave vector \mathbf{k} , components of the two-dimensional RLV, circular frequency ω , the Fourier coefficients of mass density $\rho_{\mathbf{G}}$ and components of elastic stiffness tensor $C_{\mathbf{G}}^{ijmn}$. n is the total number of RLV used in the Fourier expansion and $\mathbf{U} = [A_{\mathbf{G}}^1, A_{\mathbf{G}}^2, A_{\mathbf{G}}^3]^T$ is the displacement vector. The expressions of the matrices are listed in Ref.[18, 19].

Eq. (5) is more complicated than that of the two-dimensional phononic crystal with cubic symmetry given by Tanaka and Tamura [7] in such a way that the coefficient matrix \mathbf{B} is not vanished. However, it can be solved by introducing $\mathbf{V} = k_z \mathbf{U}$ and rewritten in the form as [9]

$$\begin{bmatrix} \mathbf{0} & \mathbf{I} \\ -\mathbf{A}^{-1}\mathbf{C} & -\mathbf{A}^{-1}\mathbf{B} \end{bmatrix} \begin{bmatrix} \mathbf{U} \\ \mathbf{V} \end{bmatrix} = k_z \begin{bmatrix} \mathbf{U} \\ \mathbf{V} \end{bmatrix} \quad (6)$$

Bulk and Surface Waves in 2-D Phononic Crystals

It is worth noting that the case of bulk wave is a special case of Eq. (5). When k_z in Eq. (5) is equal to zero, the equation degenerates into the eigenvalue problem of bulk waves as

$$\mathbf{C}\mathbf{U} = \mathbf{0} \quad (7)$$

The dispersion relations of bulk waves propagating in two-dimensional phononic crystals with both the filling material and the background material belong to the triclinic system; can be obtained by setting the determinant of matrix \mathbf{C} equal to zero.

For material with symmetry higher (and equal to) than orthorhombic symmetry, the matrix \mathbf{C} can be decoupled into two different polarization modes as

$$\begin{bmatrix} M_{\mathbf{G},\mathbf{G}'}^{(1)} - \omega^2 R_{\mathbf{G},\mathbf{G}'}^{(1)} & L_{\mathbf{G},\mathbf{G}'}^{(1)} \\ L_{\mathbf{G},\mathbf{G}'}^{(2)} & M_{\mathbf{G},\mathbf{G}'}^{(2)} - \omega^2 R_{\mathbf{G},\mathbf{G}'}^{(2)} \end{bmatrix} \begin{bmatrix} A_{\mathbf{G}'}^1 \\ A_{\mathbf{G}'}^2 \end{bmatrix} = 0 \quad (8)$$

for mixed polarization modes (i.e., longitudinal (L) and shear horizontal (SH)) and

$$\left[M_{\mathbf{G},\mathbf{G}'}^{(3)} - \omega^2 R_{\mathbf{G},\mathbf{G}'}^{(3)} \right] \left[A_{\mathbf{G}'}^3 \right] = 0 \quad (9)$$

for shear vertical (SV) modes with polarization of the displacement along the z direction (i.e., the filler's length direction). The expressions of the components in Eqs.(8) and (9) are listed in Ref.[18, 19].

It is worth noting that for material with symmetry lower than orthorhombic symmetry, the matrix \mathbf{C} can't be decoupled into two different polarization modes. The full matrix \mathbf{C} must be considered and distinguish different modes as quasi shear vertical modes, quasi shear horizontal modes and quasi longitudinal modes.

For the case of surface wave, the $6n$ eigenvalues $k_z^{(l)}$ of Eq. (6) are the apparent wave numbers of the plane waves in the z direction. According to the exponential dependence of z in Eq. (4), the real part of $k_z^{(l)}$ denotes the plane wave propagation in the z direction, and a positive nonvanishing imaginary part represents attenuation in the z direction. For surface waves propagate in a half space ($z > 0$), only $3n$ eigenvalues, which attenuate in the positive z direction are chosen, i.e., $\text{Im}(k_z^{(l)}) > 0$. Accordingly, the surface wave displacement can be expressed as

$$\begin{aligned} \mathbf{u}(\mathbf{r}, t) &= \sum_{\mathbf{G}} e^{i(\mathbf{k}+\mathbf{G})\cdot\mathbf{x}-i\omega t} \left(\sum_{l=1}^{3n} \mathbf{A}_{\mathbf{G}} e^{ik_z^{(l)}z} \right) \\ &= \sum_{\mathbf{G}} e^{i(\mathbf{k}+\mathbf{G})\cdot\mathbf{x}-i\omega t} \left(\sum_{l=1}^{3n} X_l \boldsymbol{\varepsilon}_{\mathbf{G}}^{(l)} e^{ik_z^{(l)}z} \right) \end{aligned} \quad (10)$$

where $\boldsymbol{\varepsilon}_{\mathbf{G}}^{(l)}$ is the associated eigenvector of the eigenvalue $k_z^{(l)}$. The prime of the summation denotes that the sum over \mathbf{G} is truncated up to n . X_l is the undetermined weighting coefficient which can be determined from the traction free boundary conditions on the surface $z = 0$, i.e.,

$$\mathbf{T}_{i3} |_{z=0} \equiv C_{i3mn} \partial_n \mathbf{u}_m |_{z=0} = 0 \quad (i=1,2,3) \quad (11)$$

Substituting Eq. (10) into (11), we have

$$\begin{bmatrix} H_{1,\mathbf{G}}^{(1)} & H_{1,\mathbf{G}}^{(2)} & \cdots & H_{1,\mathbf{G}}^{(3n)} \\ H_{2,\mathbf{G}}^{(1)} & H_{2,\mathbf{G}}^{(2)} & \cdots & H_{2,\mathbf{G}}^{(3n)} \\ H_{3,\mathbf{G}}^{(1)} & H_{3,\mathbf{G}}^{(2)} & \cdots & H_{3,\mathbf{G}}^{(3n)} \end{bmatrix} \begin{bmatrix} X_1 \\ X_2 \\ \vdots \\ X_{3n} \end{bmatrix} \equiv \tilde{\mathbf{H}}\mathbf{X} = 0 \quad (12)$$

where $\tilde{\mathbf{H}}$ is a $3n \times 3n$ matrix and its components are listed in Ref.[18, 19].

For the existence of a nontrivial solution of X_l , the following condition must be satisfied, i.e.,

$$\det(\tilde{\mathbf{H}}) = 0 \quad (13)$$

Eq. (13) is the dispersion relation for surface waves propagating in two-dimensional phononic crystals with both the filling material and the background material belong to the triclinic system. The relative magnitude of the eigenvectors X_l can be obtained by substituting k_z and ω , which satisfy Eq. (13), into Eq. (12).

Numerical Examples

The Fourier coefficients, $\rho_{\mathbf{G}}$ and $C_{\mathbf{G}}^{ijmn}$ in Eqs. (2) and (3), can be expressed as

$$\alpha_{\mathbf{G}} = \begin{cases} \alpha_A f + \alpha_B (1-f) & \text{for } \mathbf{G} = 0 \\ (\alpha_A - \alpha_B) F_{\mathbf{G}} & \text{for } \mathbf{G} \neq 0 \end{cases} \quad (14)$$

where $\alpha = (\rho, C^{ijmn})$, f is the filling fraction that defines the cross-sectional area of a cylinder relative to a unit-cell area, and $F_{\mathbf{G}}$ is called the structure function defined as

$$F_{\mathbf{G}} = \frac{2fJ_1(Gr_0)}{Gr_0} \quad (15)$$

with $J_1(x)$ a first order Bessel function.

In this paper, phononic structures with square lattice and hexagonal lattice are considered. These lattices are consisting of circular cylinders (A) embedded in a background material (B) forming two-dimensional lattices with lattice spacing a as shown in Fig. 1a (square lattice) and Fig. 1b (hexagonal lattice). Figs. 2a and 2b are the Brillouin regions of the square lattice and the hexagonal lattice, respectively. In the square lattice, the reciprocal lattice vector is $\mathbf{G} = (2\pi N_1/a, 2\pi N_2/a)$, where $N_1, N_2 = 0, \pm 1, \pm 2, \dots$ and filling fraction is $f = (\pi r_0^2)/a^2$. For anisotropic materials, the irreducible part of the Brillouin zone of a square lattice is shown in Fig. 2a, which is a square with vertexes Γ, X, M, Y . The reciprocal lattice vector of a hexagonal lattice is $\mathbf{G} = (2\pi N_1/a, 2\pi(2N_2 - N_1)/\sqrt{3}a)$, where $N_1, N_2 = 0, \pm 1, \pm 2, \dots$ and filling fraction is $f = (2\pi r_0^2)/\sqrt{3}a^2$. The irreducible part of the Brillouin zone of a hexagonal lattice is shown in Fig. 2b, which is a quadrangle with vertexes Γ, K, L, Y . The elastic properties of the materials utilized in the following examples are adopted from Ref.[17].

In this paper, we consider a phononic structure consisting of circular cylinders of Al embedded in a background material of Y-cut barium sodium niobate forming a two-dimensional hexagonal lattice. The material of the filling cylinders is isotropic aluminum and the base material is barium sodium niobate with orthorhombic symmetry. In the following calculations, the x-z plane is parallel to the (001) plane and the x-axis is parallel to the [100] direction of barium sodium niobate. The filling fraction is $f = 0.6$.

Shown in Figure 3 are the dispersion curves of the bulk modes and surface acoustic modes of the Al/Barium sodium niobate (Y-cut) phononic structure with hexagonal lattice. The vertical axis is the normalized frequency $\omega^* = \omega a/C_l$ and the horizontal axis is the reduced wave number $k^* = ka/\pi$. As the elastic waves propagate along the x axis, the nonvanishing displacement of the shear horizontal mode, shear vertical mode and longitudinal mode are $u_y, u_z,$ and u_x respectively. For the

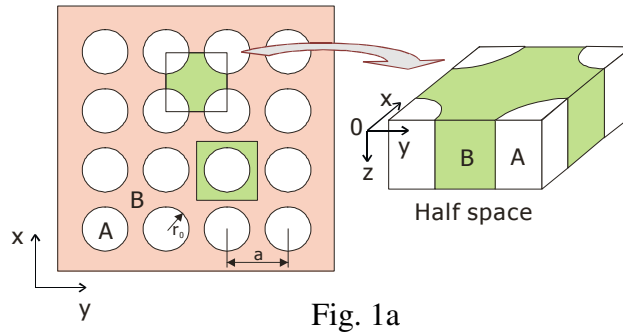


Fig. 1a

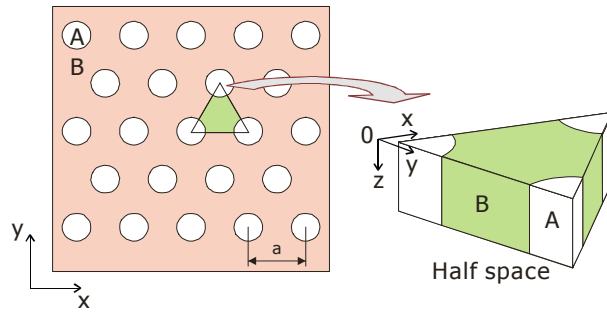


Fig. 1b

Fig. 1. Phononic structures with square lattice (1a) and hexagonal lattice (1b)

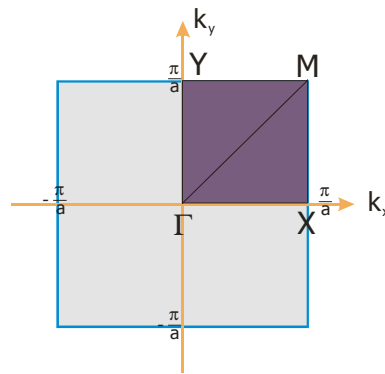


Fig. 2a

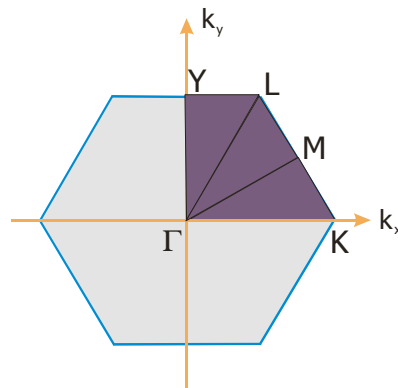


Fig. 2b

Fig. 2. Brillouin zone of the square lattice (2a) and the hexagonal lattice (2b)

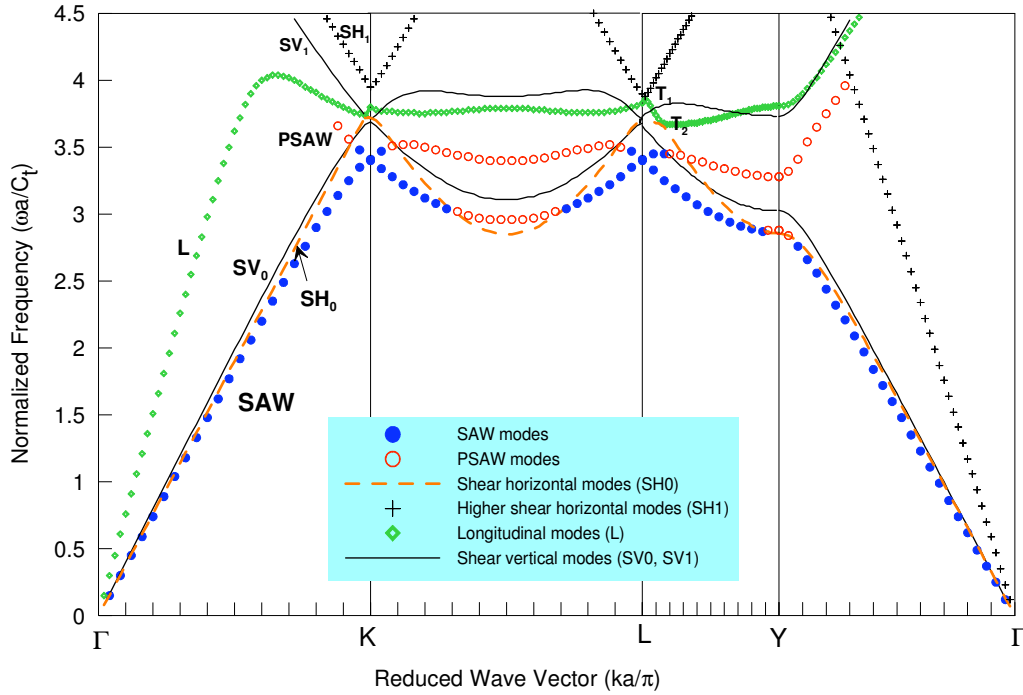


Fig. 3. Dispersion Relations of BAW & SAW modes (Al/Barium sodium niobate (Y-cut), $f = 0.6$, Hex.)

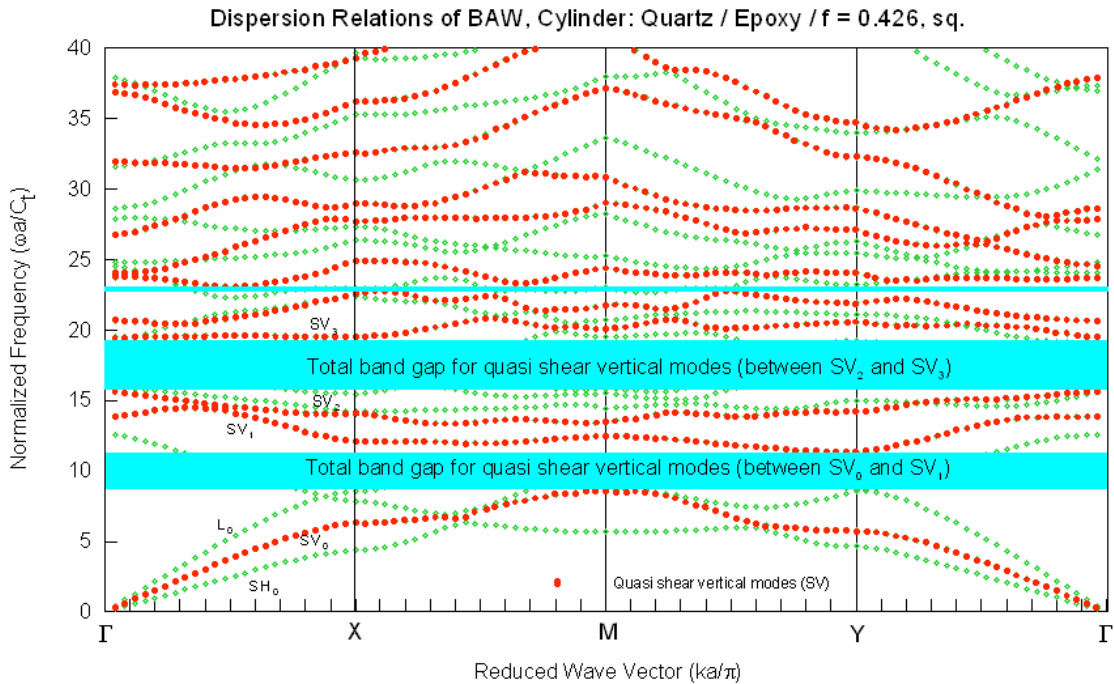


Fig. 4. Dispersion Relations of BAW modes (Quartz/Epoxy, $f = 0.426$, Sq.)

sequence modes appear, we distinguish the same type mode as the fundamental, the first and the second modes et al. For example in Figure 3, the thin solid lines represent the SV bulk acoustic modes (the fundamental mode is SV_0 and the first mode is SV_1), and the square symbols are those for the longitudinal mode (L). The thin dashed line represents the fundamental shear horizontal mode SH_0 , while the lines with “+” symbols represent the first shear horizontal mode SH_1 . The longitudinal modes L are shown as square symbols. It is seen that the dispersion relations in K-L section are almost symmetric respect to the center of the section (M point in Fig.2(b)). It is worth noting that in the L-Y section, sharp bends of the dispersion curves occur between SH_1 and L modes (T_1 point) and between

L and SH₀ modes (T₂ point). Therefore, there are mode conversions (SH and L) exist in this phononic structure with hexagonal lattice.

From Figure 3, the solid circles represent the dispersion relations of the surface wave modes (SAW) and the open circles are those for the pseudo-surface wave (PSAW) modes. For the convenience in discussing the interaction of the surface wave and bulk wave, the dispersion of the surface and bulk modes are shown in the same figure. Result showed that as the normalized frequency of the surface wave mode lies between the SH₀ and SH₁ modes, the surface wave degenerates into the pseudo-surface wave mode. Unlike the normal surface wave mode, the displacement of the pseudo-surface wave mode does not decay to zero at large depth. In the present case, one finds that at K point, there is no surface wave band gap existed. However, along the Γ -Y boundary, a PSAW-PSAW band gap exists at the boundary point Y. The phenomenon showed the characteristics of an anisotropic material.

In the second example, we consider a phononic structure consisting of quartz circular cylinders embedded in a background epoxy material of forming a two-dimensional square lattice with lattice spacing a . Figure 4 shows the dispersion relations of all bulk waves along the boundaries of the irreducible part of the Brillouin zone with filling ratio $f=0.426$. For the quartz cylinders, the matrix \mathbf{C} in Eq. (7) can't be decoupled into mixed polarization modes and transverse polarization modes. The similar modes for the different polarizations in this phononic structure are distinguished as quasi shear vertical modes, quasi shear horizontal modes and quasi longitudinal mode. In Figure 4, the vertical axis is the normalized frequency and the horizontal axis is the reduced wave number propagating along full Brillouin zone of a square lattice shown in Figure 2(a). The square symbols represent the quasi longitudinal modes and quasi shear horizontal modes. The solid circles represent the dispersion relations of quasi shear vertical modes. We can find that there are three total band gaps between quasi SV₀ and quasi SV₁, between quasi SV₂ and quasi SV₃, and between quasi SV₄ and quasi SV₅ in the normalized frequency range $\omega^* = 0 \sim 40$.

Conclusion

In this paper, we studied the phononic band gaps of surface waves and bulk waves in two-dimensional phononic structures consisted of general anisotropic materials. The explicit formulations of the plane harmonic bulk wave and the surface wave dispersion relations in such a general phononic structure are derived based on the plane wave expansion method. Al/Barium sodium niobate (Y-cut) phononic structure with hexagonal lattice and Quartz/Epoxy phononic structure with square lattice are considered in the numerical examples. Total band gap characteristics of the phononic structures with anisotropic materials are calculated and discussed. It is worth noting that some of the crossing over of the dispersion curves (apparently) is indeed sharp bends of the dispersion curves. Around this sharp bend area, the mode exchange suddenly. Results of this paper can serve as a basis for both numerical and experimental investigations of phononic crystal structures consisted of general anisotropic materials.

Acknowledgments

The authors thank the financial supports of this research from the National Science Council of Taiwan, Academia Sinica of Taiwan and the NTU-ITRI center.

References

- [1] C.M. Soukoulis, "Photonic Band Gaps and Localizations," Plenum, New York. (1993).
- [2] J.D. Joannopoulos, R.D. Meade, and J.N. Winn, "Photonic Crystals," Princeton University Press, Princeton, NJ. (1995).

- [3] T. Aono and S. Tamura, *Phys. Rev. B* 58, 4838, (1998).
- [4] R.E Vines, J.P. Wolfe, and A. G. Every, *Phys. Rev. B* 60, 11871, (1999).
- [5] R.E Vines and J.P. Wolfe, *Physica B* 263-264, 567, (1999).
- [6] A.G. Every, R.E. Vines and J.P. Wolfe, *Phys. Rev. B* 60, 11755, (1999).
- [7] Y. Tanaka and S. Tamura, *Phys. Rev. B* 58, 7958, (1998).
- [8] Y. Tanaka and S. Tamura, *Phys. Rev. B* 60, 13 294, (1999).
- [9] M.S. Kushwaha, P. Halevi, L. Dobrzynski, and B. Djafari-Rouhani, *Phys. Rev. Lett.* 71, 2022, (1993).
- [10] M.S. Kushwaha, P. Halevi, G. Martinez, L. Dobrzynski, and B. Djafari-Rouhani, *Phys. Rev. B* 49, 2313, (1994).
- [11] M. Kafesaki and E.N. Economou, *Phys. Rev. B* 60, 11993, (1999).
- [12] D. Garica-Pablos, M. Sigalas, F.R. Montero de Espinosa, M. Kafesaki and N. Garcia, *Phys. Rev. Lett.* 84, 4349, (2000).
- [13] I.E. Psarobas and N. Stefanou, *Phys. Rev. B* 62, 278, (2000).
- [14] Zhengyou Liu, C.T. Chan, and Ping Sheng, *Phys. Rev. B* 62, 2446, (2000).
- [15] Jun Mei, Zhengyou Liu, Jing Shi, and Decheng Tian, *Phys. Rev. B* 67, 245107, (2003).
- [16] J.H. Wilkinson, “**The algebraic eigenvalue problem,**” Clarendon Press, Oxford. (1965).
- [17] B.A. Auld, “Acoustic Fields and Waves in Solids,” Volume I, 2nd edition, Robert E. Kreiger, Malabar, Florida. (1990).
- [18] S. Lin, “A Study on Frequency Band Gap in Two-dimensional Phononic Crystals,” Master Thesis, Institute of Applied Mechanics, National Taiwan University, (2001).
- [19] Tsung-Tsong Wu, Zi-Gui Huang and S. Lin, “Surface and bulk acoustic waves in two-dimensional phononic crystal consisting of materials with general anisotropy,” *Phys. Rev. B*, to be published, (2004).

Advances in Nondestructive Evaluation

doi:10.4028/0-87849-948-2

**Analyses of Elastic Waves in Aluminum/Barium Sodium Niobate and Quartz/Epoxy
Phononic Structures**

doi:10.4028/0-87849-948-2.1119